Benzo[c]quinolizin-3-ones Theoretical Investigation: SAR Analysis and Application to Nontested Compounds

S. F. Braga* and D. S. Galvão

Instituto de Física Gleb Wataghin, Universidade Estadual de Campinas, C.P. 6165, CEP 13083-970, Campinas -S.P., Brazil

Received May 18, 2004

We investigate with the use of theoretical methodologies the activity of a set of 41 benzo[*c*]quinolizin-3-ones (BC3), some of them explored as selective inhibitors of the human 5α-reductase steroid. For the structure−activity study we have considered dividing the molecules into groups of tested and nontested compounds. Semiempirical calculations and pattern recognition methods such as Electronic Indices Methodology (EIM), Principal Components Analysis (PCA), Hierarchical Cluster Analysis (HCA), and K−Nearest Neighbors (KNN) have been applied to search for a correlation between experimental activity and theoretical descriptors. Our results show that it is possible to directly correlate some molecular quantum descriptors with BC3 biological activity. This information can be used in principle to identify active/inactive untested compounds and/or to design new active compounds.

1. INTRODUCTION

The manifestation of some human diseases such as benign prostatic hyperplasia (BPH)[1−3] and prostatic carcinoma[4−6] and skin disorders such as acne,[7,8] pattern baldness in men,[9,10] and hirsutism in women[11,12] are currently associated with the excessive dihydrotestosterone (DHT) production in the human body. The DHT is a metabolite originated by a stereoselective reduction of the male hormone testosterone catalyzed by the 5α-reductase (5AR) steroid.[13] In this way the inhibition of 5AR is considered a solution to control the DHT production without changes in testosterone levels.

The 5AR is a family of two isoenzymes, named 5AR1 and 5AR2, not equally distributed in the human tissues and with distinct biochemical and pharmacological properties.[14,15] Although the precise role of each isoenzymes in diseases is not yet fully understood, this division could allow a selective therapeutic inhibition of the 5ARs in an effort to control specific diseases.

5AR1 is present in the scalp, skin, and liver, and its inhibition would be a therapeutic approach to skin disorders of men suffering from alopecia or acne and women suffering from hirsutism and polycystic ovarian syndrome.[16] The 5AR1 inhibitors are an option in the treatment of women because of the well-known risks of pseudohermafroditism for a male fetus associated with 5AR2 blockade in pregnant women.[1,17]

5AR2 is distributed over the prostate and genital skin, and its inhibition was initially considered as a treatment to BPH. The Finasteride drug marked by Merck (PROSCAR) was applied as the first selective inhibitor to 5AR2.[18] It was observed however that only 30−40% of the treated cases were successfully controlled.[19,20] In this case, the BPH treatment of both 5AR1 and 5AR2 inhibition became necessary,[16] and a new compound, Dutasderide, was developed by Glaxo[21] (AVODART) to be used in this form.

During the last two decades a great effort has been made in the development and identification of potent 5ARs inhibitors.[11,22] Many of these compounds are based on the steroidal structure of testosterone with modifications in the A or B rings such as 4-azasteroids, 6-azasteroids, 19-nor-10-azasteroids, pyridones, benzophenones, benzoquinones, benzoquinolones, and benzoquinolinones.[23−29]

In this work we have investigated a series of 41 benzo-[*c*]quinolizin-3-ones (BC3)[30,31,16] (Table 1, Figure 1), some of them presenting selective 5AR1 inhibitory properties. These compounds are structurally related to some benzoquinolines, which are potent inhibitors of 5AR1.[32,33]

We have carried out semiempirical calculations to obtain optimized geometries and electronic parameters to be used in association with pattern recognition methods, such as Electronic Indices Methodology (EIM),[34] Principal Components Analysis (PCA),[35] Hierarchical Cluster Analysis (HCA),[36] and K−Nearest Neighbors (KNN).[36]

The EIM method was proposed in 1996[34] correlating electronic molecular quantum descriptors and experimental biological activity of Polycyclic Aromatic Hydrocarbons (PAHs). This methodology has been able to identify through simple rules whether a specific PAHs molecule would (or would not) exhibit carcinogenic activity. PCA[35] and HCA,[36] on the other hand, are methods widely used in pattern-recognition studies. They are exploratory methods applied to select descriptors, among dozens of them, able to cluster compounds into classes of activity. The KNN[36] is a very simple multicategory evaluation procedure able to classify new samples taking into to account an analyzed training set. These methodologies are valuable tools in the rational drug design and development of new and better drugs. Structure−activity relationship studies can provide a theoretical, a priori indication of potentially active or inactive molecules and give a contribution to decrease the time and money consuming of biochemical testing of a large amount of compounds.

* Corresponding author phone: +5519 37885345; fax: +5519 37885376; e-mail: scheila@ifi.unicamp.br.

10.1021/ci049837u CCC: $27.50
Published on Web 08/25/2004

Table 1. Group of Studied Benzo[c]quinoliz-3-ones[a]

compd	unsaturation	R1	R2	R3	R4	R5	IC_{50} (nM)	compd	unsaturation	R1	R2	R3	R4	R5	IC_{50} (nM)[b]
1		H	H	H	H	H		22	1.2	H	Me(α)	H	H	H	2700 ± 300
2		H	H	H	H	Me		23	1.2	H	Me(*β*)	H	H	H	4300 ± 400
3		H	H	H	H	Cl		24	1.2	H	Me(α)	H	H	Me	137 ± 58
4		H	Me(α)	H	H	H		25	1.2	H	Me(*β*)	H	H	Me	312 ± 23
5		H	Me(*β*)	H	H	H		26	1.2	H	Me(*β*)	H	H	Cl	141 ± 24
6		H	Me(α)	H	H	Me		27	1.2	H	H	Me(α)	H	Cl	9100 ± 500
7		H	Me(*β*)	H	H	Me		29	1.2	H	H	H	Me(α)	Cl	188 ± 42
8		H	Me(α)	H	H	Cl		35	4.5	H	H	H	H	H	298 ± 75
9		H	Me(*β*)	H	H	Cl		36	4.5	H	H	H	H	Me	376 ± 185
10		H	H	Me(α)	H	Cl		37	4.5	H	H	H	H	Cl	49 ± 19
11		H	H	H	Me(α)	Me		38	4.5	H	Me	H	H	H	185 ± 62
12		H	H	H	Me(α)	Cl		39	4.5	H	Me	H	H	Me	20 ± 8
13		Me(α)	H	H	H	Cl		40	4.5	H	Me	H	H	Cl	7.6 ± 0.9
14		Me(*β*)	H	H	H	Cl		41	4.5	H	H	Me	H	Cl	346 ± 185
15		H	Me(α)	Me(α)	H	Cl		42	4.5	H	H	H	Me	Me	14.3 ± 5.9
16		H	Me(*β*)	Me(α)	H	Cl		43	4.5	H	H	H	Me	Cl	14.4 ± 3.4
17		H	Me(α)	H	Me(α)	Me		44	4.5	Me	H	H	H	Cl	204 ± 49
18		H	Me(α)	H	Me(α)	Cl		45	4.5	H	Me	Me	H	Cl	15.6 ± 4.0
19	1.2	H	H	H	H	H	5130 ± 130	46	4.5	H	Me	H	Me	Me	15.8 ± 4.6
20	1.2	H	H	H	H	Me	176 ± 17	47	4.5	H	Me	H	Me	Cl	8.5 ± 2.1
21	1.2	H	H	H	H	Cl	459 ± 118								

[a] The inhibition potency of 5AR is given by the IC_{50} index. [b] Data from ref 16.

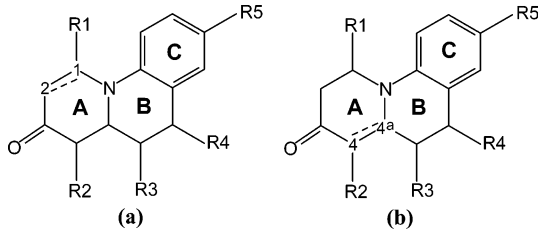

Figure 1. Structural representation of benzo[*c*]quinolizin-3-ones: (a) 4aH-series and (b) 1H-series.

Our results show that it is possible to directly correlate some molecular quantum descriptors with BC3 biological activity. This information can be used in principle to identify active/inactive untested compounds and/or to design new active compounds.

2. METHODOLOGY

The series of benzo[*c*]quinolizin-3-ones (BC3) investigated here (Table 1, Figure 1) has been synthesized and considered as selective inhibitors to 5AR1 by Guarna and collaborators.[30,31,16] They proposed that these molecules are good candidates for the development of drugs for acne, androgenic alopecia, and polycystic ovarian syndrome treatment.

The studied set is composed of a diverse group of molecules with stereochemical lateral groups bonded to a central skeleton presenting two ring unsaturation positions in the A ring. In our study we divided the BC3 set into two main groups. The first group, named Tested Group (TG), is composed of the derivatives to which the biological index IC50 has been experimentally obtained (compounds numbered from 19 to 47 in Table 1). The second group, named Nontested Group (NTG), is composed of BC3s not experimentally evaluated relative to 5AR1 inhibition (compounds numbered from 1 to 18 in Table 1).

The main structural differences between molecules of the two groups are that while TG compounds present the A ring unsaturated the NTG components present it saturated.

The TG contains 23 compounds (Table 1) divided into two subsets structurally grouped according to the A ring unsaturation position:

- 4aH series with the unsaturation between the carbons 1 and 2, molecules 19 to 29

- 1H series with unsaturation between the carbons 4 and 4a, molecules 35 to 47.

The potency of inhibition observed for the 1H molecules was verified to be greater than that of the 4aH series.[16] The remaining 18 molecules (1 to 18) of the set constitute the NTG.

For calculations of the most stable geometries of the compounds in vacuo the Austin Method 1 (AM1)[37] and Parametric Method 3 (PM3)[38,39] semiempirical results have been tested against ab initio optimized geometry for two molecules: 27 (from the 4aH series) and 42 (from the 1H series). No experimental geometric data are available in the literature for BC3s, and the selected molecules represent here models for the investigation of semiempirical calculations accuracy.

The AM1 and PM3 methods are known as an evolution to Modified Neglect of Differential Overlap (MNDO) parametrization. As the most employed semiempirical methods, they collect good and bad evaluations and divide opinions about which is the best one.[40−46]

The ab initio calculations were performed with the Titan program[47] applying a 6-31G base in a Hartree−Fock calculation and varying the improper dihedrals of the rings in steps of 120 degrees. To the semiempirical calculations no variations of angles or dihedrals were applied during the geometry optimization.

The AM1 and PM3 methods have presented high-quality results when compared to ab initio data (see next section) and encouraged us to use both of them to obtain the electronic properties of the minimized energy geometry.

Once the optimized geometries, eigenvalues, and eigenvectors have been obtained we proceed to the properties

calculation, the first being the molecular density of states (DOS).

The electronic density of states (DOS) is defined as the number of electronic states per energy unit.[48] The related concept of local density of states (LDOS) is introduced in order to also describe the spatial distribution of molecular orbitals.

For the LDOS calculations the contribution of each atom to an electronic level is weighted by the square of the (real) molecular orbital coefficient summed over the selected atomic orbitals (n_I to n_f).[34,49−51]

This corresponds to a discrete modulation and allows a direct comparison of DOS and LDOS calculated from any LCAO method.

Once calculated the DOS and LDOS then carry out the structure−activity relationship analysis (SAR) using the EIM methodology.[34]

EIM uses very simple Boolean rules based on the concept of LDOS and critical energy values for two molecular orbital levels to discriminate active and inactive compounds (with relation to some specific biological activity). This approach is based on two major descriptors, named η and Δ.

η is the LDOS relative difference between the frontier molecular electronic levels calculated to a specific molecular region. Δ is defined as the energy separation of the molecular levels considered in η.

The criterion for selecting molecular regions for the LDOS analysis considers that these regions should be present in all BC3s and be of chemical significance (sites with attached groups, preferential sites for electrophilic/nucleophilic attacks, binding or docking regions, etc.).

The EIM concept has been employed with success in classificatory problems of hundreds of compounds of different molecular systems.[34,49−51,57]

The EIM obtained results have been contrasted with pattern recognition multivariate methods used in SAR studies such as Principal Component Analysis (PCA),[35,58] Hierarchical Cluster Analysis (HCA),[36] and K−Nearest Neighbor (KNN).[36]

PCA is an extremely useful explorative tool. It considers dozens of theoretical properties (descriptors) and aims to select the ones that are capable of separating the molecules (samples) into subsets according to their experimental activity indices.

PCA maps samples through scores and individual descriptors by the loadings in a new vector space defined by the principal components (PC). In a geometrical interpretation, the set of descriptors of each molecule defines its geometrical position (a molecule-point) in an *n*-dimensional space, where each descriptor corresponds to an axis of this space. Score plots allow sample identification, clarifying whether they are similar or dissimilar, typical or outliers. From loading plots the most important descriptors can be easily identified as well as the correlation patterns among them.

HCA, also an exploratory tool, is used to validate the molecular grouping previously identified by PCA. The primary goal of HCA is to emphasize the natural grouping of similar samples based on their proximity in the multidimensional space spanned by the used variables. The results, qualitative in nature, are presented in the form of a dendogram, allowing the visualization of clusters and correlation among samples. In HCA, the distances (Euclidean metric) between the samples are calculated and transformed into a similarity matrix whose elements are the similarity indices ranging from zero to one; a smaller distance means a larger index.

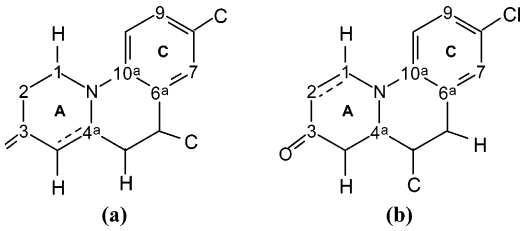

Figure 2. Structural representation of compounds 42 (a) and 27 (b) and atom labeling considered in Table 2(a)−(c).

The KNN method is a very simple procedure of classification of new samples (without experimental data) according to a previously analyzed training set. The method is based on the measurement of the distance (Euclidian) between a new sample and its neighbors in the training set. This distance is calculated over molecules distributed in the *n*-dimensional space constructed in PCA analyses. Considering the K nearest neighbors, the new sample is classified in the subset of the training set with the majority of neighbors.

Summed to the method simplicity is the advantage of being a multicategory evaluation, allowing the classifications of a new sample among more than 2 subsets in the training set.

In the next section we present the results obtained by the four methods to TG and their application in the prediction of activity of NTG compounds.

3. RESULTS AND DISCUSSIONS

3.1. Tested Group. The set of studied BC3s presents IC_{50} experimental indices varying from 7.6 to 9100 (nM). To the structure−activity-relationship (SAR) investigation the compounds of TG were divided into two subgroups of activities, where active (*A*) molecules present inhibition power measured by $IC_{50} \leq 1000$, and inactive (*I*) molecules present inhibition power of $IC_{50} > 1000$ (IC_{50} in nM).

3.1.1. Geometry Optimization. The choice of the best semiempirical method for BC3s optimization preceded our activity investigation. Table 2(a)−(c) and Figure 2 present the bond lengths, bond angles, and dihedrals obtained from PM3 and AM1 optimizations contrasted against ab initio 6-31G results. The molecules (4aH)27 and (1H)42 exemplify the set of studies TGs. These data, analyzed in conjunction with Table 3 of the root-mean-square deviation (RMS), showed that the semiempirical optimized geometries were satisfactory. The deviations of bond lengths and bond angles are very small when compared to ab initio global minimum, while the dihedral discrepancies are a little larger but localized.

As can be seen from Table 3 the RMS deviations were comparable for the two semempirical methods, the difference in the dihedral angle being smaller and in favor of AM1 (1.838 degrees to the molecule 42 and 0.966 degrees to the molecule 27). Having in mind these results we proceed with the study using the two semiempirical methods in order to investigate some dependence of the structure−activity results with the semiempirical parametrization.

3.1.2. Structure−Activity Investigation. 3.1.2.1. EIM Method. All the theoretical quantum descriptors were

Table 2. Theoretical Calculated (a) Bond Lengths, (b) Bond Angles, and (c) Bond Dihedrals of the Molecules 42 and 27[a]

	42			27		
atoms	6-31G	PM3	AM1	6-31G	PM3	AM1
			(a) Bond Lengths (Å)			
1-2	1.523	1.520	1.525	1.388	1.344	1.355
2-3	1.515	1.515	1.505	1.462	1.471	1.459
3-4	1.457	1.471	1.454	1.518	1.513	1.505
3-3O	1.200	1.219	1.238	1.198	1.219	1.237
4-4a	1.346	1.353	1.365	1.529	1.529	1.532
4a-5	1.508	1.496	1.504	1.540	1.543	1.545
4a-11	1.377	1.428	1.393	1.467	1.497	1.467
5-6	1.533	1.526	1.522	1.538	1.530	1.525
6-6a	1.513	1.499	1.494	1.518	1.492	1.487
6a-7	1.308	1.393	1.393	1.392	1.397	1.398
7-8	1.393	1.394	1.397	1.379	1.389	1.394
8-9	1.383	1.396	1.398	1.386	1.394	1.398
9-10	1.388	1.386	1.389	1.380	1.387	1.389
10-10a	1.387	1.402	1.412	1.391	1.402	1.412
10a-11	1.414	1.441	1.409	1.418	1.454	1.422
11-1	1.458	1.491	1.449	1.375	1.424	1.395
5-5CH3				1.530	1.520	1.513
6-6CH3	1.535	1.522	1.517			
			(b) Bond Angles (deg)			
1-2-3	111.96	111.17	113.14	120.37	121.62	121.19
2-3-4	114.15	116.25	115.25	114.18	115.79	114.78
2-3-3°	121.82	121.58	121.19	123.99	122.46	123.63
3-4-4[a]	122.33	122.82	122.51	113.74	113.76	114.30
4-4a-5	121.04	120.45	119.03	116.82	112.85	113.01
4-4a-11	123.07	120.58	122.30	109.45	111.17	112.40
4a-5-6	111.07	113.63	113.26	107.45	109.73	108.84
5-6-6[a]	106.87	110.35	110.25	114.35	114.54	114.35
6-6a-7	122.06	119.67	120.09	119.88	118.38	118.41
6-6a-10[a]	118.46	120.61	119.94	121.50	122.43	121.99
6a-7-8	122.41	120.79	121.22	120.62	119.98	120.42
7-8-9	117.30	119.31	118.78	120.82	120.96	120.35
8-9-10	121.49	120.52	121.12	118.91	119.49	119.84
9-10-10[a]	120.54	120.35	120.40	120.69	120.02	120.56
10-10a-11	121.87	121.05	121.74	120.12	118.61	119.81
10a-11-1	119.63	117.94	119.36	118.52	114.66	117.06
10a-11-4[a]	120.98	118.61	120.31	115.24	114.15	115.05
4a-5-5CH3				114.02	111.54	112.29
5-6-6CH3	112.68	111.70	111.29			
7-8-8CH3	120.83	120.47	120.87			
			(c) Dihedral Angles (deg)			
1-2-3-4	−34.99	−29.99	−32.98	−9.54	−13.07	−14.68
1-2-3-3°	174.63	151.22	149.58	173.59	168.53	167.77
2-3-4-4[a]	7.28	4.35	11.98	35.88	34.82	35.34
3-4-4a-5	−174.61	−180.96	−179.33	73.3	78.98	83.07
3-4-4a-11	6.21	−2.11	1.43	−49.96	−46.35	−44.38
4-4[a]-5-6	140.81	150.1	149.7	172.48	175.12	172.45
4-4[a]-11-1	10.84	26.9	8.47	39.69	38.01	33.18
4a-5-6-6a	57.2	46.54	46.56	39.07	38.97	39.41
5-6-6a-10a	−36.55	−31.98	−31.38	−8.59	−10.48	−10.87
5-6-6a-7	141.28	148.4	148.33	172.7	188.92	170.37
6-6[a]-7-8	−177.63	−180.7	−179.5	179.48	178.21	179.11
6-6a-10a-11	−3.75	−3.14	−2.36	0.67	0.33	−0.92
7-8-9-10	−0.75	0.1	−0.41	−0.2	0.32	0.02
8-9-10-10a	−0.66	0.13	−0.67	1.22	0.16	0.16
9-10-10a-11	−178.11	−176.32	−177.68	−180.39	−178.75	−178.09
10-10a-11-1	11.62	−13.9	7.72	−60.25	−62.64	−55.91
4-4a-5-5CH3				50.06	53.93	51.35
4a-5-6-6CH3	−67.01	−76.74	−77.08			
6a-7-8-8CH3	−178.42	−179.32	−179.09			

[a] The atom labeling follows Figure 2.

obtained from the molecules already optimized. To get the LDOS contributions and the descriptor η to EIM analysis, the molecules skeleton were divided into four regions (Figure 1):

- Region 1 (*R1*) − composed of the A ring;
- Region 2 (*R2*) − composed of the N_{11} (nitrogen) atom;
- Region 3 (*R3*) − composed of the C_{4a} (carbon) atom;
- Region 4 (*R4*) − composed of the C ring.

Table 3. Global Root Mean Square of Lengths, Angles, and Dihedrals, Comparing ab Initio and Semiempirical Geometries

		root mean square		
molecule		bond length	bond angle	dihedral angle
42	6-31G/AM1	0.022	0.317	1.838
	6-31G/PM3	0.023	0.403	2.472
27	6-31G/AM1	0.004	0.331	0.966
	6-31G/PM3	0.005	0.428	1.158

The N11 atom was explicitly chosen because it is the only heteroatom in the molecular skeletons. The C4a atom, on the other hand, corresponds to the target site in testosterone reduction to dihydrotestosterone and gives information about a possible mimetic action of BC3s in the 5AR inhibition process. The rings A and C had been selected because they are the regions of the molecular skeletons most exposed to biochemical reactions.

To the EIM investigation we considered the electronic parameters:

- HOMO (Highest Occupied Molecular Orbital), LUMO (Lowest Unoccupied Molecular Orbital), HOMO-1 and LUMO+1 energies;
- the energy intervals ΔH = HOMO−HOMO-1 and ΔL = LUMO+1-LUMO;
- the LDOS to the orbitals HOMO, HOMO-1, LUMO, and LUMO+1, relative to the R1, R2, R3, and R4 molecular regions (C(H), C(H-1), C(L), and C(L+1));
- the difference in LDOS distribution to each region above (ηH=[C(H)-C(H-1)], e ηL= [C(L+1)-C(L)]).

After an exploratory search involving these parameters we observed that the descriptors corresponding to HOMO and HOMO-1 exhibit the greatest correlations with the experimental inhibition index for BC3s.

In Table 4 we present the (AM1 and PM3) ΔH and ηH data for the 4 molecular regions mentioned above. The data are displayed considering the decrease of inhibition power of molecules (increasing of IC_{50}).

It is interesting to notice that to the BC3s studied set it is possible to correlate the inhibition activity with the parameters of 3 out of 4 investigated molecular regions (R1, R2, and R4). The critical values of Δ and η (ΔHc and ηHc) obtained to separate active and inactive compounds are presented in Table 5. We can observe that they differ very little (only by 0.1) when calculated with different semiempirical methods. This is a very positive result and it indicates that, in the BC3s study, the EIM parameters are not dependent on the applied semiempirical method. We propose that this behavior occurs as a consequence of the rigidity and small dimensions (compared to other drugs) of the BC3s, where the local minimum geometries are close to the global minimum.

As can be observed and dissimilar to other EIM studies, each electronic parameter (Δ and η) alone is able to separate the molecules according to their biological activity. As a consequence, four rules involving only one parameter can be constructed to classify BC3s. All the rules obey a simple *IF THEN* logic (Table 6).

In Table 7 we summarize the results of these rules applied over the values of the parameters presented in Table 4. As can be observed, the rules derived for the isolated electronic parameters present few errors in the prediction of the

Table 4. Electronic EIM Variables Δ and η Calculated with AM1 and PM3 Methods[a]

		AM1					PM3				
molecules	IC_{50} (nM)	ΔH	ηH_R1	ηH_R2	ηH_R3	ηH_R4	ΔH	ηH _R1	ηH _R2	ηH _R3	ηH _R4
40	7.6	1.374	0.513	0.534	0.005	−0.333	1.299	0.506	0.635	−0.006	−0.083
47	8.5	1.395	0.504	0.535	0.004	−0.327	1.304	0.437	0.643	−0.016	−0.001
42	14.3	1.435	0.633	0.535	0.011	−0.551	1.432	0.982	0.708	0.027	−0.935
43	14.4	1.446	0.369	0.526	−0.018	−0.224	1.363	0.325	0.573	−0.032	0.116
45	15.6	1.264	0.391	0.533	−0.004	−0.213	1.119	0.417	0.639	−0.011	−0.053
46	15.8	1.408	0.524	0.535	0.006	−0.410	1.420	0.656	0.716	−0.005	−0.539
39	20	1.382	0.561	0.535	0.009	−0.436	1.395	0.776	0.699	0.011	−0.656
37	49	1.419	0.440	0.526	−0.010	−0.297	1.329	0.368	0.572	−0.024	0.039
24	137	1.121	0.880	0.536	0.041	−0.804	1.097	1.131	0.746	0.043	−1.045
26	141	1.119	0.631	0.508	0.017	−0.529	0.969	0.561	0.555	0.003	−0.179
20	176	1.116	0.874	0.531	0.041	−0.801	1.066	1.106	0.735	0.041	−1.021
38	185	1.391	0.876	0.562	0.035	−0.774	1.374	1.078	0.738	0.032	−0.985
29	188	1.187	0.611	0.509	0.016	−0.504	1.006	0.601	0.573	0.005	−0.181
44	204	1.372	0.431	0.539	−0.009	−0.283	1.169	0.429	0.600	−0.013	−0.041
35	298	1.346	0.985	0.581	0.046	−0.870	1.304	1.155	0.753	0.041	−1.051
25	312	1.073	0.866	0.531	0.039	−0.790	1.035	1.094	0.733	0.038	−1.011
41	346	1.425	0.459	0.531	−0.009	−0.317	1.332	0.377	0.572	−0.024	0.028
36	376	1.399	0.691	0.535	0.018	−0.590	1.362	0.976	0.702	0.027	−0.890
21	459	1.167	0.646	0.511	0.019	−0.547	0.999	0.590	0.567	0.005	−0.193
22	2700	1.073	1.159	0.604	0.065	−1.059	1.062	1.357	0.820	0.059	−1.257
23	4300	1.022	1.151	0.602	0.061	−1.050	0.998	1.337	0.814	0.053	−1.238
19	5130	1.066	1.154	0.600	0.063	−1.056	1.031	1.348	0.814	0.057	−1.248
27	9100	1.151	0.656	0.512	0.020	−0.551	1.006	0.637	0.585	0.008	−0.231

[a] Rn refers to the four molecular regions selected to η calculation (see text for details).

Table 5. Electronic Critical Values

semiempirical method	ΔHc	ηHc_R1	ηHc_R2	ηHc_R4
AM1	1.1	1.0	0.6	−1.0
PM3	1.0	1.2	0.8	−1.1

Table 6. EIM Rules to Qualitative Classification (Active or Inactive) Constructed Separately to AM1 and PM3 Parameters

IF		AM1	PM3	THEN[a]
ΔH		≥1.1	≥1	A
ηH	R1	<1	<1.2	A
	R2	<0.6	<0.8	A
	R4	>−1	>−1.1	A

[a] *A* represents active to inhibition of 5AR.

biological activity (varying from 1 to 3 errors − boldfaced cells in Table 7). In general the rules obtained from AM1 data present fewer errors than the rules obtained from PM3 data. The same is true for the rules using the η parameter in comparison with the Δ*H* one. The parameter ηH for the three regions (R1, R2, and R4) classified 23 compounds presenting only 1 error (inactive compound 27), which represents the excellent accuracy of 96% in the reproduction of the experimental activity.

The EIM, as a tool of qualitative analysis of activity, was not initially developed with the intent of characterizing a molecule about the intensity of its activity. In the study of BC3s, however, we could observe that the electronic parameters give an indication of how active a molecule can be. Carefully analyzing the data of Table 4 we could observe distinct patterns of differentiation of compounds that can be used as an indication of the power of activity. In a second analysis we considered the BC3s divided into three classes of inhibition power:

- very active (+*A*) molecules presenting inhibition power measured by $IC_{50} \leq 100$ nM

Table 7. BC3s Molecules Classified as Active (A) or Inactive (I) According to the EIM Rules (Table 6) Derived from Semiempirical Calculated Descriptors (Table 4)[a]

		AM1				PM3			
molecules	Q. A.	ΔH	ηH_R1	ηH_R2	ηH_R4	ΔH	ηH_R1	ηH_R2	ηH_R4
40	*A*	A	A	A	A	A	A	A	A
47	*A*	A	A	A	A	A	A	A	A
42	*A*	A	A	A	A	A	A	A	A
43	*A*	A	A	A	A	A	A	A	A
45	*A*	A	A	A	A	A	A	A	A
46	*A*	A	A	A	A	A	A	A	A
39	*A*	A	A	A	A	A	A	A	A
37	*A*	A	A	A	A	A	A	A	A
24	*A*	A	A	A	A	A	A	A	A
26	*A*	A	A	A	A	**I**	A	A	A
20	*A*	A	A	A	A	A	A	A	A
38	*A*	A	A	A	A	A	A	A	A
29	*A*	A	A	A	A	**I**	A	A	A
44	*A*	A	A	A	A	A	A	A	A
35	*A*	A	A	A	A	A	A	A	A
25	*A*	**I**	A	A	A	A	A	A	A
41	*A*	A	A	A	A	A	A	A	A
36	*A*	A	A	A	A	A	A	A	A
21	*A*	A	A	A	A	**I**	A	A	A
22	*I*	I	I	I	I	I	I	I	I
23	*I*	I	I	I	I	I	I	I	I
19	*I*	I	I	I	I	I	I	I	I
27	*I*	**A**	**A**	**A**	**A**	**I**	**A**	**A**	**A**

[a] The boldface cells indicate predictions inconsistent with the experimental data.

- moderately active (*A*) molecules presenting inhibition power $100 < IC_{50} \leq 1000$ nM

- inactive (*I*) molecules presenting inhibition power $IC_{50} > 1000$ nM.

The AM1 electronic descriptors ηH for regions R1 and R4 and the PM3 descriptor Δ*H* allowed us to differentiate these three classes of activity with a few errors through rules presented in Table 8. Each AM1 rule classifies BC3s with 83% accuracy and the PM3 reaches 78% accuracy in the reproduction of the experimental data.

Table 8. EIM Rules to Three Ranges of Activity Constructed from AM1 and PM3 Parameters

IF			THEN[a]	compounds wrongly classified
PM3		≥1.3	+*A*	35, 36, 38, 41, 45
ΔH		>1 and <1.3	*A*	
		≤1.0	*I*	
AM1	R1	<0.6	+*A*	27, 41, 42, 44
ηH		≥0.6 and <1.0	*A*	
		>1.0	*I*	
	R4	> −0.5	+*A*	27, 41, 42, 44
		> −1.0 and≤ −0.5	*A*	
		≤ −1.0	*I*	

[a] +*A*, *A*, and *I* represent respectively very active, moderately active, and inactive to inhibition of 5AR.

These additional rules show the great potential of the EIM electronic parameters in the study of the biological activity of drugs. Beyond the capacity of compound classification in a binary system of activity (active or inactive), the electronic parameters seem to contain more complex information for BC3s.

To evaluate the accuracy of these results and to verify the importance of electronic parameters in the activity power of BC3s, we incorporated in our study some physicochemical and stereochemical parameters.

3.1.2.2. PCA and HCA Methods. The investigation with a great number of parameters was performed with the pattern recognition methods PCA and HCA. As can be observed from the results already obtained, EIM results and optimized geometry are very similar from AM1 and PM3 methods. As a consequence, only the AM1 descriptors will be discussed in the following results. The AM1 method has been selected considering two results: its little advantage to reproduce ab initio geometry and its accuracy in the exploratory classification of BC3s in three groups of activity.

The PCA and HCA analyses were performed with the Einsigth[59] program considering 39 relevant descriptors. This set involves the EIM parameters and other descriptors such as

- hardness, approximated as HD = (LUMO−HOMO)/2,
- Mulliken's electronegativity (M.E.), approximated as χ = −(HOMO+LUMO)/2,
- dipole momentum (D.M.),
- refractivity (RE),
- polarizability (PO),
- volume (V),
- mass (M),
- heat of formation (HF),
- coefficient of molecular partition octanol−water (log P).

PCA/HCA analyses produced many sets of molecular descriptors able to separate the BC3s into subsets of activity. We present here the results obtained with two groups of descriptors (A and B) that represent very well the parameters selected by PCA and the separations of molecules obtained after various and repeated analyses.

The set A is composed of the descriptors ΔH, ηH_R1, ηH_R3, V, and M.E., while B is composed of ΔH, ηH_R1, D.M., V, and M.E. As we can see, both groups, as well as the others obtained during the investigation, include necessarily electronic parameters. These results emphasize the relevance of electronic parameters in SAR investigations, since they are selected among tens of other descriptors. It is worth mentioning that investigations disregarding all EIM parameters were considered, and no activity separation of molecules was possible.

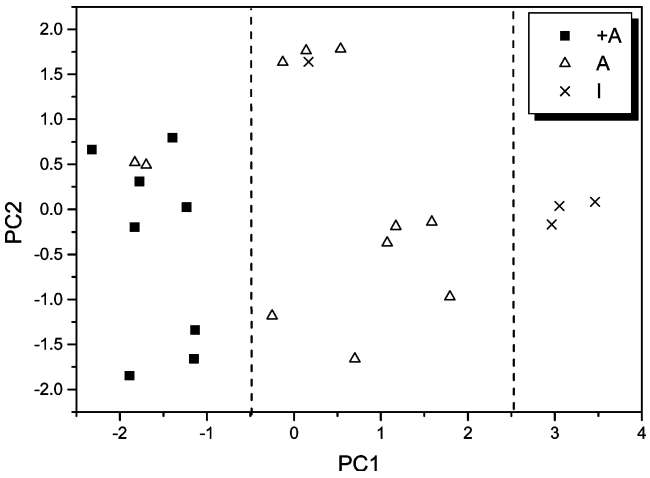

Figure 3. Plot of two PC vectors to BC3s score for the A descriptors. The compounds are separated into three subgroups as very active (+A), moderately active (A), and inactive (I).

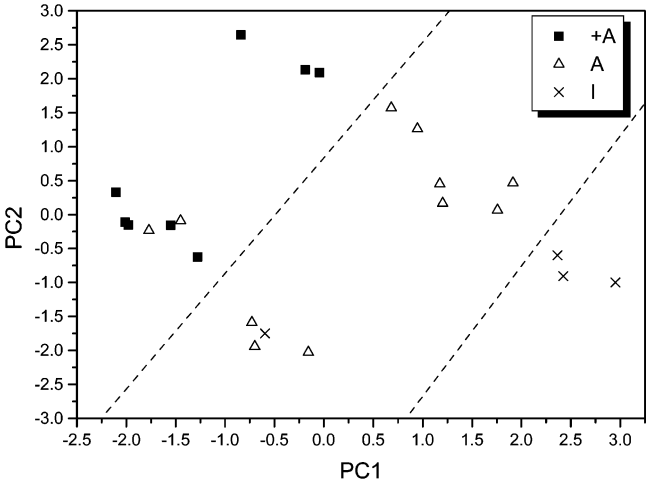

Figure 4. Plot of two PC vectors to BC3s score for the B descriptors. The compounds are separated into three subgroups as very active (+A), moderately active (A), and inactive (I).

In Figures 3 and 4 we present the score of the first two principal components (PC1 and PC2) for A and B groups of descriptors. For the two results we observe that the molecules are separated not only as active or inactive, but in three groups of inhibition potency (+A − very active, A − moderately active, and I − inactive). This separation is equivalent to the observed before, in exploratory character, for the isolated electronic parameters of EIM investigation.

The PC1xPC2 planes accumulate 85% and 83% of the variance of the system to A and B sets. The PC1 and PC2 are described by the molecular descriptors following the equations:

- Set A:

PC1 = −0.4569 ΔH + 0.5563 ηH_R1 + 0.5564 ηH_R3− 0.4148 V +0.0047 M.E.

PC2 = −0.3532 ΔH − 0.1865 ηH_R1−0.1612 ηH_R3− 0.0067 V + 0.8999 M.E.

- Set B:

PC1 = −0.3991 ΔH + 0.6123 ηH_R1 + 0.4899 D.M. − 0.4395 V − 0.1805 M.E.

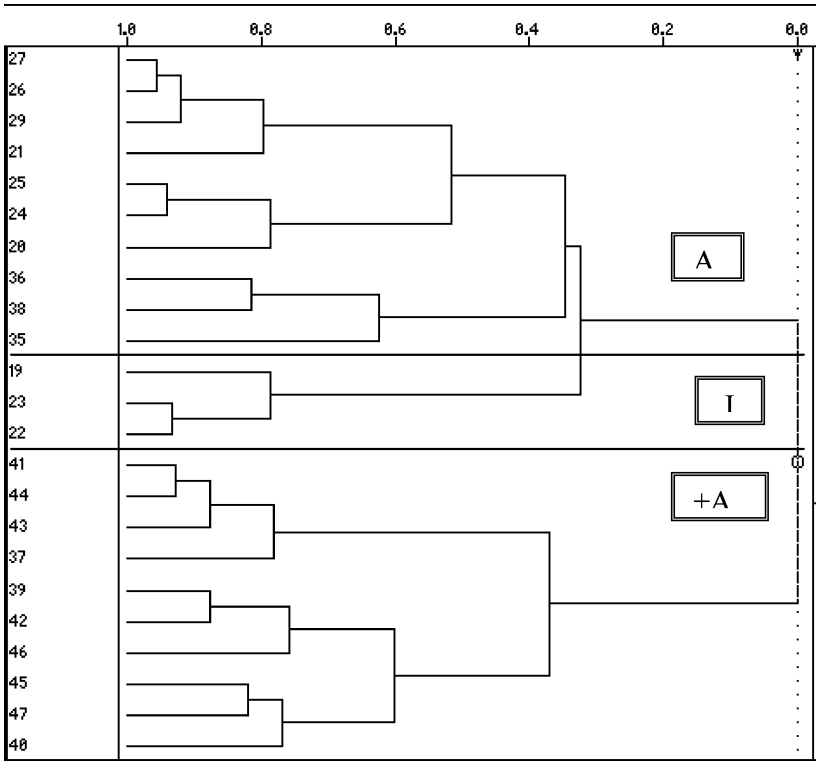

Figure 5. Dendogram of the hierarchical distribution of B3Cs for A descriptors. The very active, moderately active, and inactive compounds are clearly separated.

$PC2 = 0.4536\ \Delta H - 0.0897\ \eta H\_R1 + 0.4418$ D.M. $+ 0.2537$ V $- 0.7257$ M.E.

We can observe from Figure 3 that for the A parameters the compounds are vertically separated, indicating that the PC1 axis is the major axis responsible for this classification. The A equations show that the molecular descriptors more contributing for PC1 formation are ηH_R1 and ηH_R3, followed by ΔH and V. For the B set, on the other hand, diagonal lines separate the groups of different activities, indicating that both PCs are responsible for the classification. In this case all the parameters are equally important for the obtained results.

The PCA results present three compounds wrongly classified. The moderately active molecules 41 and 44 were classified as very active, and the inactive molecule 27 was classified as moderately active. This result is equivalent to an 87% accuracy in the separation of molecules according to the 5AR inhibition potency.

As can be observed, distinct methodologies, considering different groups of initial parameters, make indubitable the importance of the electronic descriptors in the theoretical investigation of BC3s activity. The extension to a greater applicability of these descriptors in SAR studies is real and could be observed in several EIM investigations.[34,49−57]

The results of the HCA for the A and B sets above are presented in Figures 5 and 6. It samples clearly as the molecules clusterizes according to their similarities. The results in the structure of dendograms were constructed on the basis of PCA distribution of compounds.

In Figure 5, set A, we observe the formation of three clusters: inactive (I), moderately active (A), and very active (+A) compounds. The I and A groups presented the small amount of 0.32 of similarity between them and no similarity with the +A group (varying from 0.0 to 1.0 in HCA). For the set B, Figure 6, three main clusters can also be detected, but they do not correspond directly to the three groups of activity. In fact, the I group disconnects two clusters mixing active compounds with different intensities of activity.

The patterns and rules of classification of activities obtained in this first part of the study for the TG can be used in the investigation of activity of new BC3s. Based on these results we propose to classify in the next section the biological activity of a series of BC3s not yet experimentally evaluated.

3.2. Nontested Group. The NTG molecules (1 to 18 in Table 1) form a class for which no information about the inhibition potency to 5AR is available. In the literature they are compared to the 19-nor10-azasteroids derivatives. The 19NAZs, presenting the A ring saturated, showed the IC_{50} index greater than 100000 nM. This result led to the interpretation that unsaturations in the A ring would be required to the biologic activity of 19NAZs.[25] It also suggested that the inactivity due to the absence of unsaturations in the A ring would have to be observed in the derivatives of BC3s, denoting that all the compounds in the NTG group would have to present IC_{50} around 100000 nM and be completely inactive.[25]

However, compound 8 (Table 1) is a counter example for this initial suggestion. Presenting the A ring completely saturated, the compound has IC_{50} equal to 478 nM,[16] which is comparable to that measured in compounds 25 (312 nM), 41 (346 nM), 36 (376 nM), and 21 (459 nM) of the TG, and is very inferior to that obtained for the derivatives of the 19NAZ. In conformity with our qualitative division of activity compound 8 is a moderately active compound ($100 > IC_{50} < 1000$).

Besides the cited evidences, other studies indicate that the absence of unsaturations in the A ring not necessarily leads

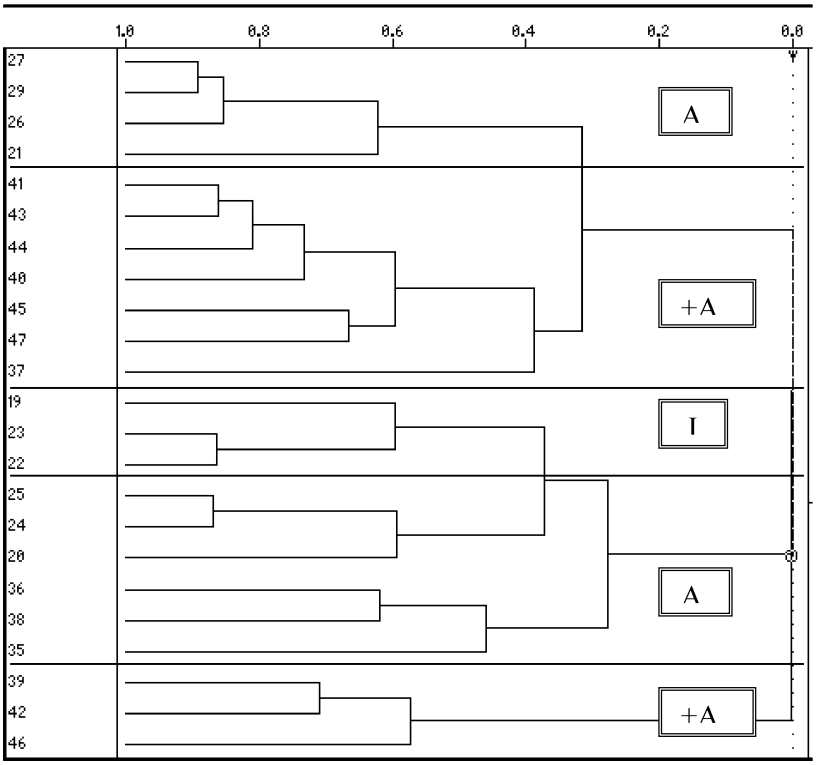

Figure 6. Dendogram of the hierarchical distribution of B3Cs for B descriptors. The active and inactive compounds are clearly separated.

to the inactivity of 5AR enzyme inhibition. For the 4-aza-steroids with inhibiting activity of enzyme 5AR1, no increase in IC_{50} was observed for compounds with the A ring saturated.[23]

This contradiction in the interpretation of the inhibition potency of NTG molecules increased our interest in the study of their theoretical classification of activity. Our proposal is that 19NAZ results cannot be directly applied to BC3s derivatives. Supporting this assumption is the analysis of the influence in activity of conjugations in the C ring. The two groups of compounds have distinct changes in 5AR inhibition potency related to the presence/absence of double bonds in the C ring.[60]

3.2.1. Structure−Activity Investigation. 3.2.1.1 EIM Method. To examine the 5AR inhibition potency of the NTG molecules, we applied the rules and patterns constructed in the TG investigation with descriptors calculated with the AM1 method (Table 6).

Considering that the accuracy of the rules for ηH descriptors is the same for the molecular regions R1, R2, and R4, we simultaneously analyzed the results for the three regions.

Table 9 presents the descriptors calculated for NTG. In a general way, the values obtained are in the same range of that calculated for the TG compounds. Analyzing separately each region (Rn) and applying the rules of Table 6, the activities of compounds are proposed.

For the region R1 all the compounds present ηH values inferior to 1 (the largest equals to 0.711 for compound 5), which indicates that all NTG compounds must be active. For ηH_R2 only compound 5 presents the ηH above 0.6 being considered inactive in our analysis and guessed to present $IC_{50} > 1000$ nM. All the remaining compounds are classified as active. For the region R4 all the compounds present ηH superior to -1 and must present IC_{50} less than 1000 nM.

Table 9. EIM Electronic Descriptors Calculated to Nontested Molecules from AM1 Method

molecule	ηH_R1	molecule	ηH_R2	molecule	ηH_R4
13	0.5127	13	0.4437	7	−0.5682
9	0.5321	7	0.4612	2	−0.5784
7	0.5330	9	0.4642	13	−0.5901
2	0.5400	2	0.4691	11	−0.6069
10	0.5410	10	0.4745	9	−0.6130
3	0.5426	3	0.4749	10	−0.6205
12	0.5500	12	0.4842	3	−0.6269
11	0.5590	11	0.4867	12	−0.6425
14	0.5650	14	0.5033	1	−0.6500
8	0.6040	8	0.5437	4	−0.6593
15	0.6330	15	0.5491	14	−0.6595
1	0.6360	6	0.5510	6	−0.6711
16	0.6370	17	0.5596	17	−0.6889
6	0.6380	18	0.5624	8	−0.6934
17	0.6473	1	0.5653	5	−0.6975
18	0.6477	16	0.5683	15	−0.7039
4	0.6571	4	0.5728	16	−0.7223
5	0.7110	5	0.6101	18	−0.7301

For the R1 region it is also possible to explore the intensity of activity more carefully applying the rules derived in Table 8. In accordance with these rules the compounds 2, 3, 7, 9, 10, 11, 12, 13, and 14 will present $IC_{50} < 100$ nM, while the remaining will present IC_{50} greater than 100 nM but below 1000 nM. To the equivalent rule for region R4 (Table 8) it is not possible to select active compounds.

The activity classification of the NTG molecules (and mainly of the activity intensity), according to parameters and rules of the EIM, preserves the experimental pattern observed for the increasing of activity of BC3s due to inclusion of a methyl or a chlorine group at specific positions of the molecular skeleton.[16] As can be observed in the results of Table 9, compound 2 (with methyl group in position 8) and compound 3 (with chlorine in position 8) present a greater power of inhibition of enzyme 5AR1 than compound 1 (with

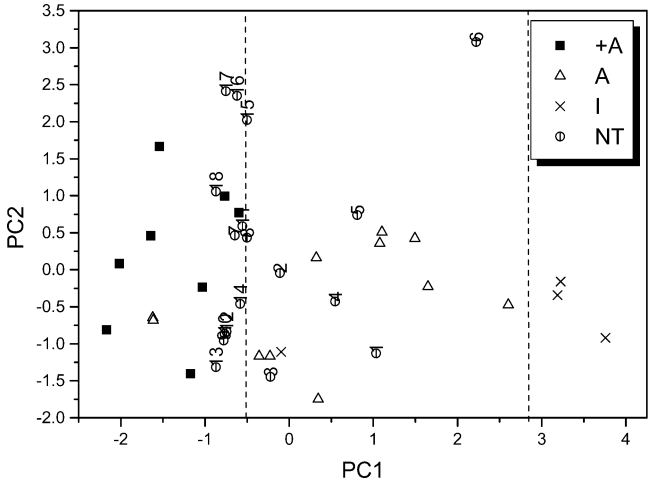

Figure 7. Plot of two PC vectors to tested and nontested BC3s score for the descriptors A.

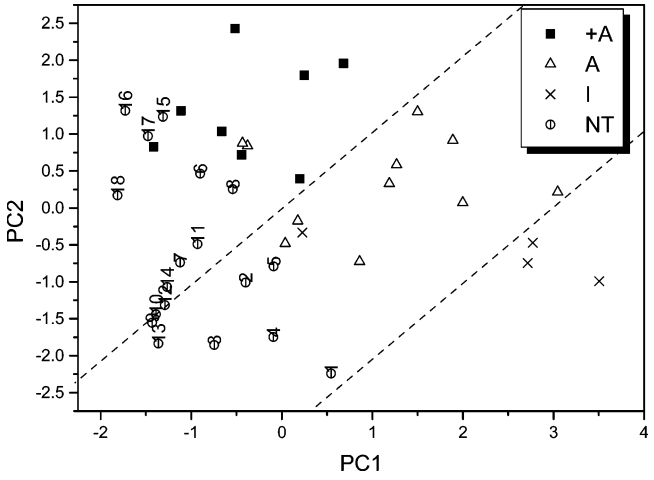

Figure 8. Plot of two PC vectors to tested and nontested BC3s score for the descriptors B.

hydrogen in position 8). The same occurs with compounds 6, 8, and 4 and compounds 7, 9, and 5.

We conclude from EIM analysis that of 18 compounds of NTG, 9 will present experimental IC_{50} inferior to 100 nM (compounds 2, 3, 7, 9, 10, 11, 12, 13, 14), 8 will present $100 > IC_{50} < 1000$ nM (compounds 1, 4, 6, 8, 15, 16, 17, 18), and only 1 will be inactive with IC_{50} greater that 1000 nM (compound 5).

3.2.1.2. PCA Method. We have also investigated the activity of the NTG molecules through the PCA methodology. PCA is classified in the chemometrics as an exploratory technique and presents limitations when applied in a classification scheme (suggestion) of molecular activity. In these particular studies, PCA results can only verify if a nontested compound possesses, in a general way, the characteristics of groups already tested.

Figures 7 and 8 present the 41 studied compounds (23 of TG and 18 of the NTG) projected in the principal components space PC1 x PC2 (PCs in a general way) constructed with the parameters previouslly selected from TG investigation (Figures 3 and 4).

We can observe from figures that the TG and NTG compounds are merged. The NTG compounds show great affinity with active molecules (+A and A), and only molecules 6 (Figure 7) and 1 (Figure 8) moved toward the region of inactive molecules but did not make part of this group.

Table 10. KNN Proposed NTG Molecules Activity for Set A and B of Descriptors Selected by PCA of TG

molecules	set A	set B
NTG Proposed Biological Activity[a]		
1	A	I
2	A	A
3	A	A
4	A	A
5	A	+A
6	A	+A
7	A	A
8	A	+A
9	A	A
10	A	A
11	A	A
12	A	A
13	A	A
14	A	A
15	+A	+A
16	+A	+A
17	+A	+A
18	+A	+A

[a] *+A*, *A*, and *I* represent respectively very active, moderately active, and inactive to inhibition of 5AR.

With the insertion of new samples in the group investigated by PCA, the equations describing PCs axis in the descriptors space became the following:

- Set A:

$PC1 = -0.1661\ \Delta H + 0.63848\ \eta H\_R1 + 0.58586\ \eta H\_R3 - 0.4624\ V - 0.0875\ M.E.$

$PC2 = 0.19659\ \Delta H + 0.0354\ \eta H\_R1 + 0.1612\ \eta H\_R3 - 0.50918\ V - 0.7806\ M.E.$

- Set B:

$PC1 = 0.10322\ \Delta H + 0.59088\ \eta H\_R1 + 0.5704\ D.M. - 0.5515\ V + 0.10287\ M.E.$

$PC2 = 0.7587\ \Delta H - 0.1051\ \eta H\_R1 + 0.40654\ D.M. + 0.39249\ V - 0.3067\ M.E.$

More specifically the PCA analysis showed that all compounds of the NTG will be active, with 1, 2, 3, 4, 5, 6, and 13 moderately active and the remaining presenting $IC_{50} < 100$ nM.

As a third activity evaluation of NTG molecules, we considered the results of KNN (K−Nearest Neighbors) analysis.

3.2.1.3. KNN Method. The KNN considers the activity of a molecule monitoring who are its neighbors in a PCA molecular distribution. For the optimization of the number of neighbors we considered as a training group the TG compounds and predicted the activity of them one at a time, observing a series of K neighbors. The optimized training prediction, for descriptors A and B, selected K equals to 4 as the best number of neighbors to be monitored, with 70% accuracy in the experimental activity reproduction.

In Table 10 we present the KNN proposed activity to NTG molecules. The results to descriptors A suggest that all the molecules will be active, while descriptors B suggest that only the molecule 1 will be inactive. This is in agreement with the EIM and PCA previous analyses, where a great majority of compounds are proposed to present biological activity between excellent and moderate.

Table 11. Summary of Classification of NTG Compounds by Pattern Recognition Methodologies

molecules	EIM-ηH_R1	EIM-ηH_R2	EIM-ηH_R4	PCA-*A*	PCA-*B*	KNN-*A*	KNN-*B*	proposed activity[a]
1	A	a	a	A	A	A	I	*I*
2	+A	a	a	A	A	A	A	*A*
3	+A	a	a	A	A	A	A	*A*
4	A	a	a	A	A	A	A	*A*
5	A	I	A	A	A	A	+A	*I*
6	A	a	a	A	+A	A	+A	*A*
7	+A	a	a	+A	+A	A	A	+*A*
8	A	a	a	a	+A	A	+A	*a*
9	+A	a	a	+A	a	A	A	*a*
10	+A	a	a	+A	+A	A	A	+*A*
11	+A	a	a	+A	+A	A	A	+*A*
12	+A	a	a	+A	+A	A	A	+*A*
13	+A	a	a	+A	A	A	A	*A*
14	+A	a	a	+A	+A	A	A	+*A*
15	A	a	A	a	+A	+A	+A	+*A*
16	A	a	A	+A	+A	+A	+A	+*A*
17	A	a	A	+A	+A	+A	+A	+*A*
18	A	a	A	+A	+A	+A	+A	+*A*

[a] +*A*, *A*, and *I* represent respectively very active, moderately active, and inactive to inhibition of 5AR, while *a* represents that no information about the intensity of inhibition could be defined to the active compound.

Table 11 sumarizes all the information of activity proposed for the NTG. Collecting the results of all the methodologies, we observed that only the NTG compounds 1 and 5 received an indication of inactivity and will be considered inactive in our classification. Compound 4 was the only one classified for unanimity by the methodologies as a moderately active compound. Disregarding the classification of the parameters ηH_R2 and ηH_R4 (as they do not present quantitative selectivity in the activity), we can consider the intensity of activity of remainder molecules. Observing the results of the 5 analyses, we consider a classification for votes, where a sum of at least 3 indications is necessary to classify a compound with a specific intensity of activity. The results are presented in the last column of Table 11.

In accordance with our final result, for 18 compounds of the NTG:

- 2 (1 and 5) will present the $IC_{50} > 1000$ nM,

- 5 (2, 3, 4, 6, and 13) will be moderately active with $100 > IC_{50} < 1000$ nM,

- 9 (7, 10, 11, 12, 14, 15, 16, 17, and 18) will be very active with $IC_{50} < 100$,

- 2 (8 and 9) will be active, but without a specific quantitative classification.

In conclusion, we have studied 41 derivatives of the benzo[*c*]quinoliz-3-ones separated into two groups of tested and nontested compounds. Our results showed that the EIM analyses is not semiempirical method dependent indicating that the classification of activity of benzo[*c*]quinolizin-3-ones is reproducible for different semiempirical methods. Applying the EIM, PCA, HCA, and KNN methodologies we were able to construct rules and patterns of classification of the molecules according to their biological activity. These rules were applied in the study of activity of 18 untested molecules proposing their activity.

REFERENCES AND NOTES

(1) Imperato-McGinley, J.; Gerrero, L.; Gautier, T.; Peterson, R. E. Steroids 5α-Reductase Deficiency in Man: an Inherited Form of Male Pseudohermaphroditism. *Science* **1974**, *186*, 1213−1215.

(2) Geller, J. Benign Prostatic Hyperplasia − Pathogenesis and Medical Therapy. *J. Am. Geriatr. Soc*. **1991**, *39*, 1208.

(3) Clifford, G. M.; Farmer, R. D. T. Medical Therapy for Benign Prostatic Hyperplasia: A Review of the Literature. *Eu. Urol*. **2000**, *38*, 2−19.

(4) Gormley, G. J. 5α-Reductase Inhibitors in Prostate Cancer. *Endocrine-Related Cancer* **1996**, *3*, 57−63.

(5) Lamb, J. C.; Levy, M. A.; Johnson, R. K.; Isaacs J. T. Response of Rat and Human Prostatic Cancers to the Novel 5-Alpha-Reductase Inhibitor, SK-and-F 105657. *Prostate* **1992**, *21*, 15−34.

(6) Njar, V. C. O.; Kato, K.; Nnana, I. P.; Grigoryev, D. N.; Long, B. J.; Brodie, A. M. H. Novel 17-Azolyl Steroids, Potent Inhibitors of Human Cytochrome 17α-Hydroxylase-$C_{17,20}$-lyase($P450_{17\alpha}$). *J. Med. Chem.* **1998**, *41*, 902−912.

(7) Thiboutot, D.; Bayne, E.; Thorne, J.; Gilliland, K.; Flanagan, J.; Shao Q.; Light, J.; Helm, K. Immunolocalization of 5α-Reductase Isozymes in Acne Lesions and Normal Skin. *Arch. Dermatol*. **2000**, *136*, 1125−1129.

(8) Sansone, G. L.; Reisner, R. M. Differential Rates of Conversion of Testosterone to Dihydrotestosterone in Acne and in Normal Human Skin − Possible Pathogenic Factor in Acne. *J. Invest. Dermatol*. **1971**, *56*, 366−372.

(9) Hogan, D. J.; Chamberlain, M. Male Pattern Baldness. *South Med. J.* **2000**, *93*, 957−662.

(10) Dallob, A. L.; Sadick, N. S.; Unger, W.; Lipert, S.; Geissler, L. A.; Gregoire, S. L.; Nguyen, H. H.; Moore, E. C.; Tanaka, W. K. The Effect of Finasteride, a 5alpha-reductase Inhibitor, on Scalp Skin Testosterone and Dihydrotestosterone Concentrations in Patients with Male Pattern Baldness. *J. Clin. Endocrinol. Metab*. **1994**, *79*, 703−706.

(11) Kuttenn, F.; Mowszowicz, I.; Shaison, G.; Mauvais-Jarvis, P. Androgen Production and Skin Metabolism in Hirsutism. *J. Endocrinol*. **1977**, *75*, 83−91.

(12) Frye, S. V. Inhibitors of 5α-Reductase. *Curr. Pharm. Des*. **1996**, *2*, 59−84.

(13) Anderson, S.; Russel, D. W. Strctural and Biochemical Properties of Cloned and Expressed Human and Rat Steroid 5α-Reductase. *Proc. Natl. Acad. Sci. U.S.A*. **1990**, *87*, 3640−3644.

(14) Russel, D. W.; Berman, D. M.; Bryant, J. T.; Cala, K. M.; Davis, D. L.; Landrum, C. P.; Prihoda, J. S.; Silver, R. I.; Thigpen, A. E.; Wigley, W. C. The Molecular Genetics of Steroid 5α-Reductases. *Recent Prog. Horm. Res*. **1994**, *49*, 275−285.

(15) Russel, D. W.; Wilson, J. D. Steroid 5α-Reductase: two genes; two enzymes. *Annu. Rev. Biochem*. **1994**, *63*, 25−61.

(16) Guarna, A.; Machetti, F.; Occhiato, E. G.; Scarpi, D.; Comerci, A.; Danza, G.; Mancina, R.; Serio, M. Benzo[*c*]quinolizin-3-ones: A Novel Class of Potent and Selective Nonsteroidal Inhibitors of Human Steroid 5α-Reductase 1. *J. Med. Chem*. **2000**, *43*, 3718−3735.

(17) Fratianni, C. M.; Imperato-McGinley, J. The Sindrome of 5α-Reductase Deficiency. *Endocrinologist* **1994**, *4*, 302−341.

(18) Rittmaster, R. S. Drug Therapy: Finasteride. *N. Engl. J. Med*. **1994**, *330*, 120−125.

(19) Gromley, G. J. *Biomed. Pharmacother*. **1992**, *9*, 319.

(20) Faller, B.; Farley, D.; Nick, H. FINASTERIDE − A Slow-Binding 5-Alpha-Reductase Inhibitor. *Biochemistry* **1993**, *32*, 5705.

(21) Palomino, E. GI-198745 Glaxo-Wellcome. *Curr. Opin. Cent. Periph. Nerv. Sust. Invest. Drugs* **1999**, *1*, 253−256.

(22) Abell, A. D.; Henderson, B. R. Steroidal and Nonsteroidal Inhibitors of Steroid 5α-Reductase. *Curr. Med. Chem*. **1995**, *2*, 583−597.
(23) Bakshi, R. K.; Patel, G. F.; Rasmusson, G. H.; Baginsky, W. F.; Cimis, G.; Ellsworth, K.; Chang, B.; Bull, H.; Tolman, R. L.; Harris, G. S. 4, 7*β*-Dimethyl-4-azacholestan-3-one (MK-388) and Related 4-Aza-steroids as Selective Inhibitors of Human Type 1 5α-Reductase. *J. Med. Chem.* **1994**, *37*, 3871−3874.
(24) Rasmusson, G. H. In *Annual Reports in Medicinal Chemistry*; Academic Press: 1996, Chapter 18, pp 179−188.
(25) Guarna, A.; Belle, C.; Machetti, F.; Occhiato, E. G.; Payne, A. H.; Cassiani, C.; Comerci, A.; Danza, G.; De Bellis, A.; Dini, S.; Marrucci, A.; Serio, M. 19-Nor-10azasteroids: A Novel Class of Inhibitors for Human Steroid 5α-Reductases 1 and 2. *J. Med. Chem*. **1997**, *40*, 1112−1129.
(26) Jones, C. D.; Audia, J. E.; Lawhorn, D. E.; McQuaid, L. A.; Naubauer, B. L.; Pike, A. J.; Pennington, P. A.; Stamm, N. B.; Toomey, R. E.; Hirsch, K. S. Nonsteroidal Inhibitors of Human Type I Steroid 5α-Reductase. *J. Med. Chem*. **1993**, *36*, 421−423.
(27) Hirsch, K. S.; Jones, C. D.; Audia, J. E.; Anderson S.; MaQuaid, L.; Stamm, N. B.; Naubauer, B. L.; Pennington, P. A.; Toomey, R. E. LY191704: A Selective Nonsteroidal Inhibitors of Human Steroid 5α-Reductase Type 1. *Proc. Natl. Acad. Sci U.S.A.* **1993**, *90*, 5277−5281.
(28) Kenny, B.; Ballard, S.; Blagg, J.; Fox, D. Pharmacological Options in the Treatment of Benign Prostatic Hyperplasia. *J. Med. Chem*. **1997**, *40*, 1293−1315.
(29) Kurup, A.; Garg, R.; Hansch, C. Comparative QSAR Analysis of 5α-Reductase Inhibitors. *Chem. Rev*. **2000**, *100*, 909−924.
(30) Guarna, A.; Occhiato, E. G.; Scarpi, D.; Tsai, R.; Danza, G.; Comerci, A.; Mancina, R.; Serio, M. Synthesis of Benzi[c]quinolizin-3-ones: Selective Non-Steroidal Inhibitors of Steroid 5α-Reductase 1. *Bioorg. Med. Chem. Lett.* **1998**, *8*, 2871−2876.
(31) Guarna, A.; Occhiato, E. G.; Scarpi, D.; Zorn, C.; Danza, G.; Comerci, A.; Mancina, R.; Serio, M. Synthesis of 8-Chloro-benzo[*c*]quinolizin-3-ones as Potent and Selective Inhibitors of Human Steroid 5α-Reductase 1. *Bioorg. Med. Chem. Lett.* **2000**, *10*, 353−356.
(32) Jones, C. D.; Audia, J. E.; Lawhorn, D. E.; McQauid, L. A.; Neubauer, B. L.; Pike, A. J.; Pennington, P. A.; Stamm, N. A.; Toomey, R. E.; Hirsch, K. R. Nonsteroidal Inhibitors Of Human Type-I Steroid 5-Alpha-Reductase. *J. Med. Chem*. **1993**, *36*, 421−423.
(33) Abell, A. D.; Erhard, K. F.; Yen, H.-K.; Yamashita, D. S.; Brandt, M.; Mohammed, H.; Levy, M. A.; Holt, D. A. Preparative Chiral HPLC Separation of all Possible Stereoisomers of LY191704 and LY266111 and their In Vitro Inhibition of Human Types 1 and 2 Steroid 5α-Reductases. *Bioorg. Med. Chem. Lett.* **1994**, *4*, 1365−1368.
(34) Barone, P. M. V. B.; Camilo, A.; Galvão, D. S. Theoretical Approach to Identify Carcinogenic Activity of Polycyclic Aromatic Hydrocarbons. *Phys. Rev. Lett.* **1996**, *77*, 1186−1189.
(35) Naes, T.; Baardseth, P.; Helgesen, H.; Isakson, T. Multivariate Techniques in the Analysis of Meat Quality. *Meat Sci.* **1996**, *43*, s135−s149.
(36) Beebe, K. R.; Pell, R. J.; Seasholtz, M. B. *Chemometrics - A Practical Guide*; Wiley: New York, 1998.
(37) Dewar, M. J. S.; Zoebisch, E. G.; Healy, E. F.; Stewart, J. J. P. The development and use of quantum -mechanical molecular -models. 76. AM1 − A new general -purpose quantum -mechanical molecular -model. *J. Am. Chem. So*c. **198**5, *107*, 3902.
(38) Stewart, J. J. P.; Optimization of parameters for semiempirical methods.1. Method. *J. Comput. Chem*. **1989**, *10*, 209−220.
(39) Stewart, J. J. P.; Optimization of parameters for semiempirical methods. 2. Applications. *J. Comput. Chem.* **198**9, *10*, 221−264.
(40) Abbasoglu, R.; Yilmaz, S. S. Quantum-chemical investigation of electrophilic addition of bromine to norbornadiene. *J. Mol. Liquids* **2002**, *96*−*7*, 397−407.
(41) Budyka, M. F., Zyubina, T. S.; Ryabenko, A. G. Computer Modeling of C-2 Cluster Addition to Fullerene C-60. *Int. J. Quantum Chem.* **2002**, *88*, 652−662.
(42) Lozynski M.; Rusinska-Ruszak, D. PM3 Conformations of C-13 Taxol Side Chain Methyl Ester. *Tetrahedron Lett.* **1995**, *36*, 8849−8852.
(43) Baumann, H.; Martin, R. E.; Diederich, F. PM3 Geometry Optimization and CNDO/S-CI Computation on UV/VIS Spectra of Large Organic Structures: Program Description and Application to Poly(tracetylene) Hexamer and Taxotere. *J. Comput. Chem*. **1999**, *20*, 396−411.
(44) Erdemoglu, N.; Sener, B.; Ide, S. Structural Features of Two Taxoids from Taxus Baccata L. Growing in Turkey. *J. Mol. Struct*. **2001**, *559*, 227−233.
(45) Michalski, J.; Hanuza, J.; Mączka, M.; Talik, Z.; Głowiak, T.; Szemik-Hojniak, A.; Van der Maas, J. H. Structural and Vibrational Data Obtained From Experimental (X-ray, IR and Raman) and AM1, PM3 and MNDO Semiempirical Methods for Ortho Meta and Para Nitraminopyridine N−Oxides. *J. Mol. Struct*. **2001**, *596*, 109−121.
(46) Dávila, L. Y. A.; Caldas, M. J. Applicability of MNDO Techniques AM1 and PM3 to Ring-Structured Polymers. *J. Comput. Chem*. **2002**, *23*, 1135−1142.
(47) TITAN 1.0.5. 2000 Wavefunction, Inc. http://www.wavefun.com.
(48) Levine, I. N. *Quantum Chemistry*, 4th ed.; Prentice-Hall: Englewood Cliffs, New Jersey, 1991.
(49) Barone, P. M. V. B.; Braga, R. S.; Camilo A.; Galvão, D. S. Electronic Indices from Semiempirical Calculations to Identify Carcinogenic Activity of Polycyclic Aromatic Hydrocarbons. *J. Mol. Struct*. (*THEOCHEM*) **2000**, *505*, 55−66.
(50) Vendrame, R.; Braga, R. S.; Takahata, Y.; Galvão, D. S. Structure−Activity Relationship Studies of Carcinogenic Activity of Polycyclic Aromatic Hydrocarbons Using Calculated Molecular Descriptors with Principal Component Analysis and Neural Network Methods. *J. Chem. Inf. Comput. Sci*. **1999**, *39*, 1094−1104.
(51) Vendrame, R.; Braga, R. S.; Takahata, Y.; Galvão, D. S. Structure-Carcinogenic Activity Relationship Studies of Polycyclic Aromatic Hydrocarbons (PAHs) with Pattern-Recognition Methods. *J. Mol. Struct*. (*THEOCHEM*) **2001**, *539*, 253−265.
(52) Coluci, V. R.; Vendrame, R.; Braga, R. S.; Galvão, D. S. Identifying relevant molecular descriptors related to carcinogenic activity of Polycyclic Aromatic Hydrocarbons (PAHs) using pattern recognition methods. *J. Chem. Inf. Comput. Sci*. **2002**, *42*, 1479−1489.
(53) Santo, L. L. E.; Galvão, D. S. Structure−Activity Study of Indolequinones Bioreductive Alkylating Agents. *J. Mol. Struct.* (*THEOCHEM*) **1999**, *464*, 273−279.
(54) Vendrame, R.; Coluci, V. R.; Braga, R. S.; Galvão, D. S. Structure−Activity Relationship (SAR) Studies of the Tripos Benchmark Steroids. *J. Mol. Struct. (THEOCHEM)* **2002**, *619*, 195−205.
(55) Braga, R. S.; Vendrame, R.; Galvão, D. S. Structure−Activity Relationship Studies of Substituted 17 Alpha-Acetoxyprogesterone Hormones. *J. Chem. Inf. Comput. Sci*. **2000**, *40*, 1377−1385.
(56) Cyrillo, M.; Galvão, D. S. Structure−Activity Relationship Study of Some Inhibitors of HIV-1 Integrase. *J. Mol. Struct*. *(THEOCHEM)* **1999**, *464*, 267−272.
(57) Braga, S. F. and Galvão, D. S. A Structure Activity Study of Taxol, Taxotere, and Derivatives Using the Electronic Indices Methodology (EIM). *J. Chem. Inf. Comput. Sci.* **2003**, *43*, 699−706.
(58) Massart, D. L.; Vandeginste, B. G. M.; Deming, S. N.; Michotte, Y.; Kaufman, L. In *Chemometrics: a textbook 2*; Elsevier: Chapter 21, p 369.
(59) Einsight 3.0. Infometrix, Inc. 2200 Sixth Ave, Suite 833, Seattle WA. 98121, 1991.
(60) Guarna, A.; Occhiato, E. G.; Machetti, F.; Trabocchi, A.; Scarpi, D.; Danza, G.; Mancina, R.; Comerci, A. and Serio, M. Effect of C-ring Modofications in Benzo[*c*]quinolizin-3-ones, New Selective Inhibitors of Human 5α-Reductase 1. *Bioorg. Med. Chem*. **2001**, *9*, 1385−1393.

CI049837U